Invited Paper

Terahertz wave generation based on laser-induced microplasmas

Fabrizio Buccheri * and Xi-Cheng Zhang
The Institute of Optics, University of Rochester, 275 Hutchison Road, Rochester, NY, 14627 USA
* Email: fbuccher@ur.rochester.edu

(Received June 17, 2015)

Abstract: Ambient air can be used as a THz wave emitter and/or THz sensor when ionized by femtosecond laser fields. The integration of such a plasma source and detector in terahertz time-domain techniques allows spectral measurements covering the elusive terahertz gap, further increasing the impact of those scientific tools in the study of the four states of matter. We report on a new paradigm for implementing THz plasma techniques. Specifically, we replace the use of elongated plasmas, with lengths ranging from a few mm to several cm, with sub-mm size plasmas, which we will refer to as microplasmas, obtained by focusing laser pulses with high numerical aperture microscope objectives (NA > 0.4). Those microplasmas have in fact unique properties compared to any other THz source and sensor, with the potential of enabling new and exciting applications. Specifically, a microplasma requires orders of magnitude less laser pulse energy to be created, enabling plasma-based terahertz technique to be implemented with low energy ultrafast lasers. Moreover, they offer a generation, or detection, volume with sub-wavelength size ($1\ THz = 300\ \mu m$), which could be exploited to implement near-field THz plasma techniques. In this paper we describe the experimental study of the terahertz emission from a laser-induced plasma of submillimeter size. One of the interesting phenomena is that the main direction of THz wave emission is almost orthogonal to the laser propagation direction, unlike that of elongated plasmas. Perhaps the most important achievement is that we have demonstrated that laser pulse energies lower than 1 μJ are sufficient to generate measurable terahertz pulses from ambient air. This significant decrease in the required laser energy will make plasma-based terahertz techniques more accessible to the scientific community.

Keywords: Terahertz spectroscopy, Plasmas, Photoionization, Ultrafast nonlinear optics

doi: 10.11906/TST.058-068.2015.06.07

1. Introduction

The development of terahertz (THz) techniques over the last two decades has been providing scientists with tools to study matter in the solid, liquid, gas, and plasma state [1-4]. Dynamics and equilibrium properties can be investigated with time-resolved THz spectroscopy (TRTS) [5] and THz time-domain spectroscopy (THz-TDS) [6] respectively.

The spectral coverage of those techniques is limited by the particular choice of emitters and detectors. When those are implemented with solid-state devices, such as inorganic nonlinear crystals or photoconductive antennas, the useful bandwidth of the measurements is usually limited to few THz. An alternative offering a significantly increased spectral coverage is to use gas plasmas induced by energetic femtosecond pulses as both THz source and sensor [7-12]. In fact, THz transients generated in ambient air plasmas induced by near infrared laser pulses have been reported to have spectral contents reaching up to 200 *THz* [13] and peak electric fields exceeding a few MV/cm [14].

Other advantages of gas plasmas compared to solid state devices are that there is no concern about laser-induced damage at high intensities; they provide a gradual refractive index interface to the THz radiation, as opposed to the abrupt interface of a solid material, therefore eliminating the spectral spatial filtering due to total internal reflection and the introduction of Fresnel reflections in the measurements; and they generally do not introduce sharp spectral features in the measurements.

The first published measurement of THz generation from ionized gas is attributed to Hamster and coworkers in 1993 [15]. In their pioneering experiment they focused highly energetic, 50 *mJ*, infrared pulses on a He target obtaining optical to THz conversion efficiency less than 10^{-6}.

A technique to enhance the efficiency of the generation mechanism by more than two orders of magnitude was later introduced by Cook and Hochstrasser. It consisted in ionizing the gas with an ultrafast laser field composed by the fundamental and its second harmonic [16]. The two different techniques are usually referred to as the "one-color" and "two-color" approaches, respectively.

In both cases, THz generation from the gas requires that peak intensity of the excitation laser to exceed its threshold for ionization. This implies the existence of a threshold for the laser pulse energy below which the gas does not generate measurable THz radiation. For a specific gas, this value depends on the numerical aperture (NA) of the laser focusing optics, and the laser pulse duration and wavelength. Experimental values for energy threshold reported in the literature are in the range of 30-50 μJ [17, 18]. Those levels of laser energies are only obtainable with an amplified laser system. However, the development of THz gas sources would greatly benefit if it was possible to replace the bulky and expensive amplified laser systems with cheaper and more user friendly sources, such ultrafast laser oscillators.

To address this problem we propose to study the THz emission from plasmas with submillimeter sizes created by focusing the laser excitation through high NA microscope objectives. We will refer to those as microplasmas. By doing so, the laser energy threshold can be reduced below the μJ level [19], paving the way to possible implementation of THz gas emitter and detectors with laser oscillators.

In addition those microplasmas have unique properties compared to any other THz source and sensor, with the potential of enabling new and exciting applications. Specifically, they offer a generation, or detection, volume with sub-wavelength size (1 *THz* = 300 μm), which could be exploited to implement near-field THz plasma techniques.

2. Experimental methods

In order to characterize the coherent emission of THz radiation from the microplasma, we employed an experimental setup implementing THz time-resolved detection. The conceptual schematic of the setup is depicted in Fig. 1. The laser excitation, provided by a commercial Ti:Sapphire amplified laser (100 *fs* pulse duration, 700 μJ pulse energy, 800 *nm* central wavelength, 1 *kHz* repetition rate), was split into two beams with controllable time delay (not shown in the figure).

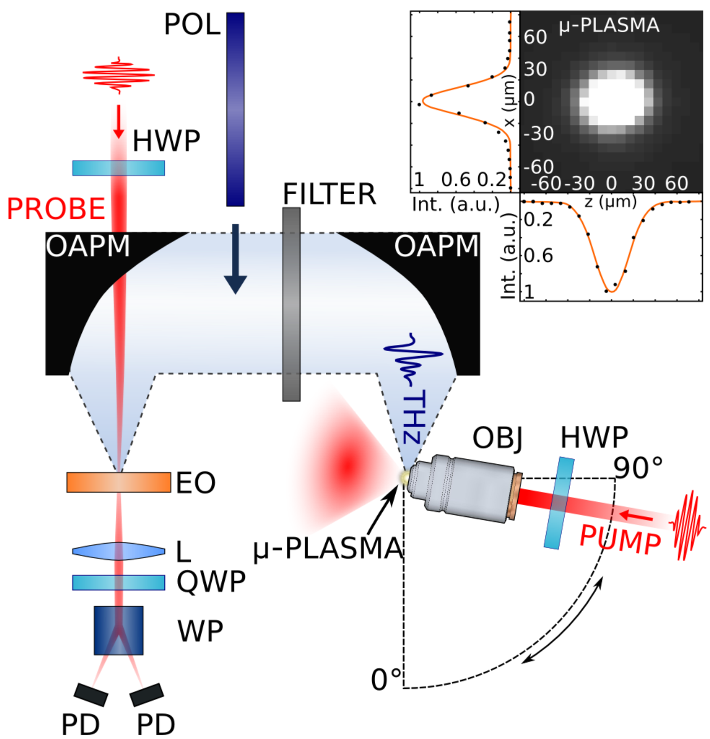

Fig. 1 Experimental setup. The pump beam is focused in ambient air with a 0.85 *NA* objective. The pump arm is, mounted on a platform, able to rotate about the position of the microplasma. In particular the detection angle, defined as the angle between the propagation direction of the pump beam and the optical axis of the collection optics, can be changed from 0 to 90 degrees. The time delay between the pump and probe pulses can be finely controlled by a mechanical delay stage (not shown in the figure). The THz and probe beams are combined together into an electro-optic crystal, which allows the retrieval of the THz waveform through the standard electro-optic technique. The inset is a picture of the microplasma created by focusing laser pulses with energy of 65 μJ through a 0.85 *NA* air-immersion objective as seen through a UV bandpass filter. Here is the list of abbreviations: HWP, half wave plate; OBJ, objective; OAPM, off-axis parabolic mirror; POL, THz polarizer; EO, electro-optic crystal; L, lens; QWP, quarter wave plate; WP, Wollaston Polarizer; PD, photo diode.

The microplasma was created by focusing the pump beam with a 0.85 *NA* microscope objective in ambient air. The polarization of the pump beam was linear and its orientation could be controlled with a half wave plate. The maximum pump pulse energy employed in the experiment was 65 μJ, limited by the damage threshold of the objective. For this excitation energy we obtained plasmas with both longitudinal and transverse sizes less than 40 μm (Fig. 1 inset). The THz radiation from the plasma source was collected and refocused with two off-axis parabolic mirrors (OAPM) of 2 inches of diameter and 3 and 2 inches effective focal length respectively. To prevent the residual pump beam to reach the detector, we placed a 2 *mm*-thick high resistivity Silicon in the THz path. We retrieved the THz waveforms by employing free space electro-optical sampling [20], where we used <110>-cut ZnTe with different thicknesses as the detectors. In particular, we opted for a thicker crystal, 3 *mm*, when we needed to increase the signal-to-noise ratio of the measurement, and for a thinner one, 0.2 *mm*, when we needed to increase the useful bandwidth.

With the aim of studying the angle-dependent emission of the source, we installed the pump section of the setup on a platform which is able to rotate about the geometrical focus of the microscope objective, which is the position of the microplasma. The apparatus was designed to minimize the optical path difference between the pump and probe arms upon rotation, so to reduce the experimental error and the user intervention.

3. Terahertz emission from the microplasma

We recorded THz waveforms for ten different detection angles ranging from 0 to 90 degrees. The detection angle is defined as the angle between the optical axis of the THz collecting mirror and the propagation axis of the pump beam. The solid angle of collection was limited by the diameter of the first off-axis parabolic mirror for all detection angles. The time-resolved field measurements as a function of detection angle, shown in Fig. 2(a), highlight that the THz emission is not collinear with the laser excitation. In our experimental conditions, the coherent emission of THz collected in the forward direction with 0 degrees, is negligible, compared to the one collected for detection angles close to 90 degrees. Specifically, the strongest THz emission was observed for a detection angle of 80 degrees.

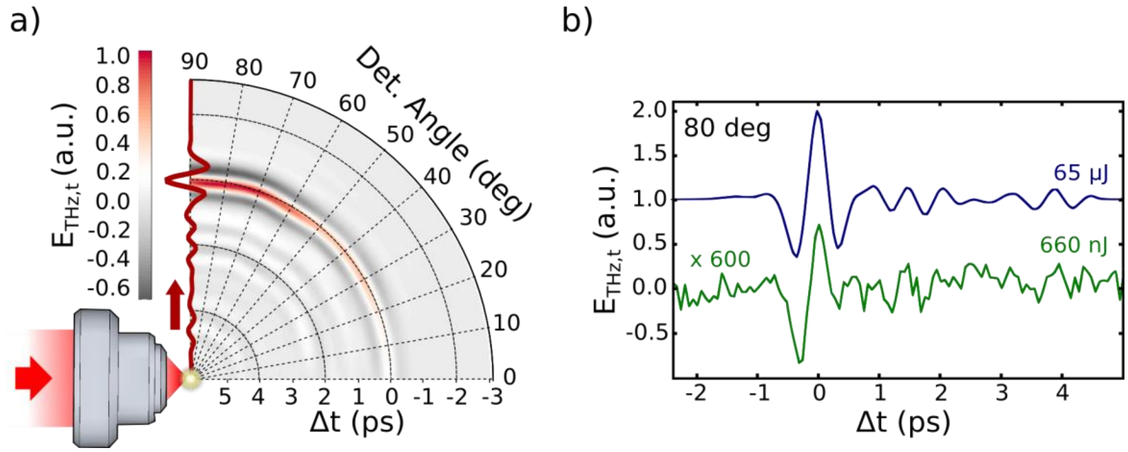

Fig. 2 (a) Density plots representing the recorded THz waveforms as a function of the detection angle. The density plots are obtained through spline interpolation of ten experimental traces measured at ten degrees intervals starting from zero degree. Δt is the time delay between the pump and the probe beam. The density plot is normalized to one respect the highest signal recorded among all the detection angles. (b) Measured THz waveforms at detection angle of 80 degrees for a laser pulse energy of 65 μJ (top) and of 660 *nJ* (bottom). For clarity, the plots are offset and the waveform measured at 660 *nJ* is magnified 600 *times*.

Typical THz waveforms measured for this value of detection angle are shown for two different pump laser pulse energies in Fig. 2(b). The waveform on the top is obtained with a laser energy of 65 μJ, which is the highest that is safe to send through the objective without causing damage to it. The waveform on the bottom is obtained with a laser energy of 660 *nJ*, which is the lowest at which we were able to record a THz waveform.

To our knowledge that is the first time that the measurement of THz radiation from ambient air is reported for sub-μJ laser excitation energies. The value of 660 *nJ* is more than one order of magnitude lower than previously reported ones [17, 18] and it is limited by the signal-to-noise ratio (SNR) of the detection system.

Fig. 3(a) shows the detected amplitude spectra computed from the measured waveforms shown in Fig. 2(a) as a function of the detection angle. Each spectrum is normalized to one such that its shape can be easily compared for different detection angles. We did not measure significant differences between the spectra as a function of angle. The spectral amplitude for a detection angle of 80 degree is depicted in Fig. 3(b) for two different thicknesses of the detection crystal. This picture shows that the emission is broadband and limited by the useful detection bandwidth of the electro-optic sampling method.

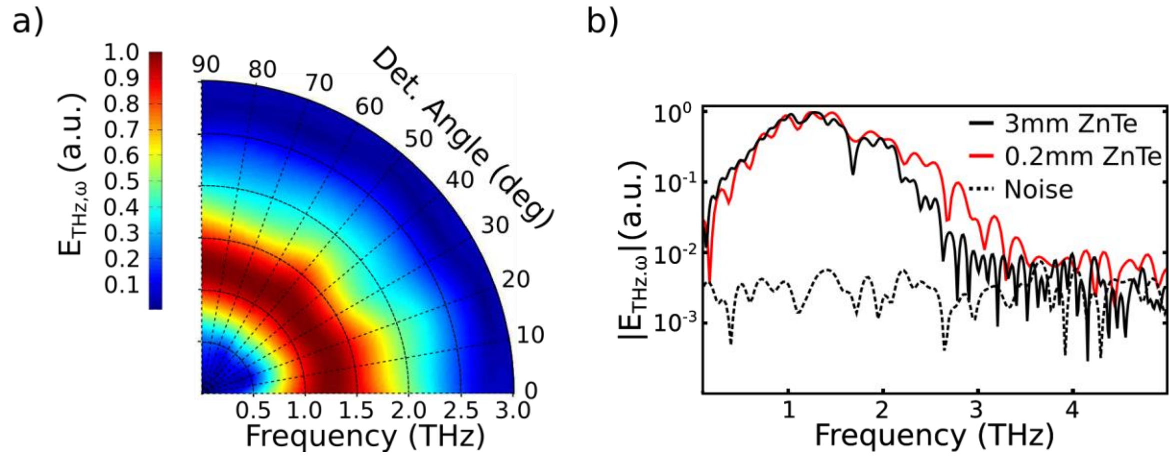

Fig. 3 a) Density plots representing the computed THz amplitude spectra as a function of the detection angle. The density plot is obtained through spline interpolation of ten computed corresponding to ten values of detection angle. Each single spectrum is normalized to one. b) Spectral amplitude of the THz waveform measured at detection angle of 80 degrees for a laser pulse energy of 65 μJ, for detector thickness of 3 *mm* (solid black) and 0.2 *mm* (solid red), and of the noise of the detector (dashed line).

The THz peak power scales with the square of the pump pulse energy, as shown in Fig. 4, independently of detection angle. The experimental data starts to deviate from the parabolic fit for pump pulse energies above 55 μJ. In our experimental conditions, we were not able to discern whether this was due to the saturation of the THz emission mechanism, or to nonlinear interactions between the intense laser pulse and the glass composing the objective, such as self-phase modulation.

Linear rotations of the optical pump polarization did not affect the measured THz emission pattern, amplitude and phase. Finally, we employed a wire grid polarizer to investigate the polarization of the detected THz radiation, see Fig. 1, exploiting the polarization sensitivity of electro-optic sampling in the same manner of [21]. Within our collection angle the measured THz waveforms were horizontally polarized independently of the pump beam polarization.

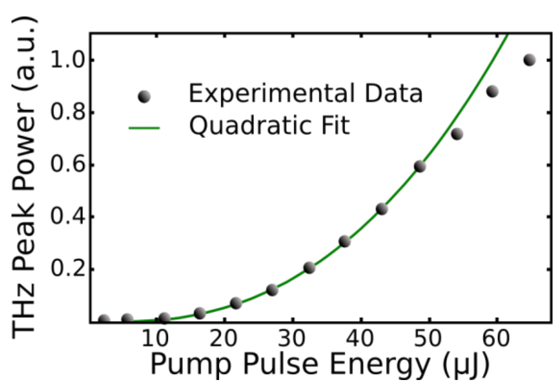

Fig. 4 THz pulse peak power vs. pump pulse energy. The detection angle was 80 degrees. The solid dots correspond to the experimental data, while the solid line is the best quadratic fit.

4. Discussion

We limited our investigation to the one-color approach. The emission of THz under this condition has been firstly studied by Hamster and coworkers, who attributed the generation mechanism to space charge separation induced by the laser ponderomotive force [15] and estimated the following scaling law for the THz peak power P_{THz} as a function of the parameters characterizing the laser [22] :

$$P_{THz} \propto \frac{(W \cdot NA \cdot \lambda)^2}{\tau^4} \tag{1}$$

where W is the laser pulse energy, NA is the numerical aperture of the focusing laser cone, λ is the laser wavelength and τ is the pulse duration. With our experimental setup, we were not able to rigorously verify the validity of this simple formula, however, the measured scaling of THz peak power as a function of the laser pulse energy was quadratic, as predicted by Eq. 1. Moreover, as a qualitative study, we repeated the measurements using two objectives with different numerical apertures, 0.65 *NA* air immersion and 1.25 *NA* oil immersion. Compared to the 0.85 *NA* air immersion objective, the 1.25 *NA* objective yielded stronger THz emission, while the 0.65 *NA* objective yielded weaker THz emission. However, it was not possible to consider it a systematic study in light of the different designs among the pieces in terms of glass dispersion and thickness, clear aperture, and aberration corrections.

The radiation pattern can be qualitatively attributed to a transient plasma current developing along the laser optical axis. The experimental findings are all consistent with the ponderomotive force being the main driver of this longitudinal plasma currents originating the emission of THz transients. This force is proportional to the local intensity gradient and therefore it is not strongly affected by polarization rotations of the linearly polarized laser field, explaining why the measured waveforms are not sensitive to them.

The longitudinal plasma current can be described with a 1D analytical model, originally proposed by D'Amico and coworkers to explain the forward THz emission from filaments within the framework of transition-Cherenkov-like emission [23].

The THz emission is calculated as the far-field radiation of a longitudinal plasma current $j_z(\omega)$. The energy spectral density emitted in the unit solid angle is [23]:

$$\frac{d^2W_{THz}}{d\omega d\Omega} \propto |j_z(\omega)|^2 f(\omega,\theta,L) \tag{2}$$

$$f(\omega,\theta,L) = \frac{\sin^2\theta}{(1-\cos\theta)^2}\sin^2\left(\frac{L\omega}{2c}(1-\cos\theta)\right) \tag{3}$$

where θ is the emission angle, L is the longitudinal length of the plasma column, and c is the speed of light.

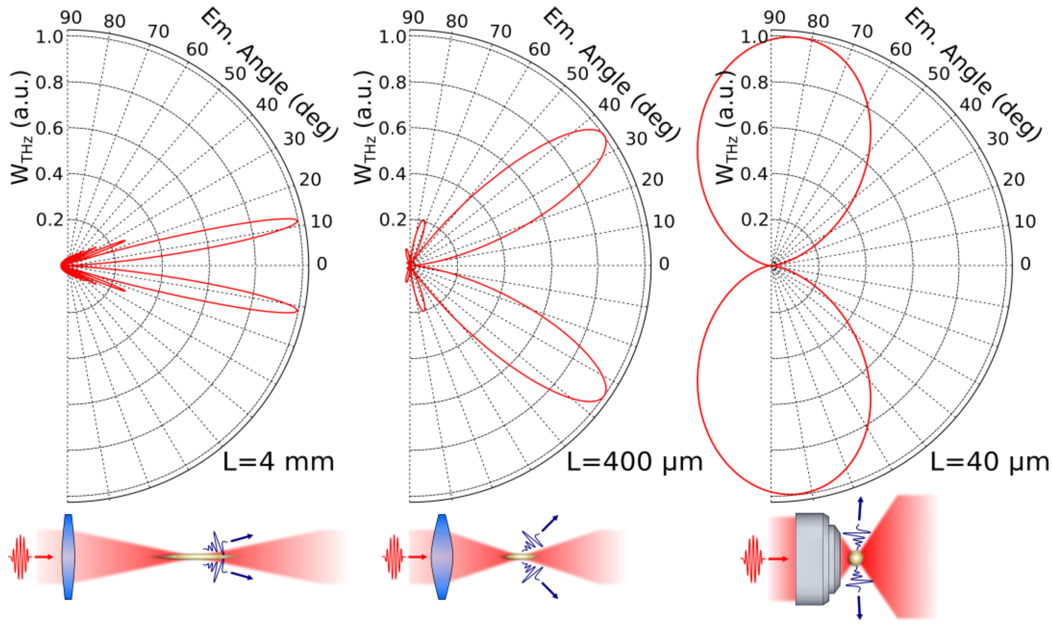

Fig. 5 Computation of THz pulse energy as a function of emission angle for three different values of plasma lengths. From left to right, the plasma length is 4 *mm*, 400 μm, and 40 μm respectively.

Fig. 5 shows, as example, the predicted radiation pattern for a frequency of 1.5 *THz* for three different plasma lengths. The THz emission is oriented in the forward direction for longer plasma length and move away from the laser optical axis as the plasma size is reduced. It is noteworthy how this simple 1D analytical model developed for very different plasma conditions, i.e., filamentation, would also qualitatively describe the radiation pattern when the length of the filament is reduced to 40 μm.

We compared the model described in Eq. (2) and Eq. (3) to our experimental measurement. The results are shown in Fig. 6. We numerically integrated Eq. 2 over the detection solid angle and the frequency interval accessible with our detection technique (0.1 to 2.5 *THz*) for each value of detection angle. We estimated the electron densities to be greater than 10^{18} cm^{-3}, corresponding to plasma frequencies higher than 9 *THz*, and electron collision frequencies much smaller than the plasma frequency. Fig. 6 shows that this simple analysis predicts the angle of maximum emission correctly, although the predicted radiation pattern is less directive than the measured one.

We found that the radiation pattern predicted by the model greatly depends on the geometrical factor $f(\omega, \theta, L)$, describing the summation in the far-field of radiation coming from a source moving at the speed of light over a finite length L, while it is only loosely affected by the spectral content of the excitation current $j_z(\omega)$, and therefore by parameters such as electron density and electron collision frequency.

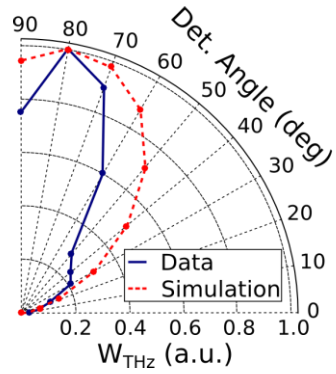

Fig. 6 THz pulse energy as a function of detection angle. The pulse energy is computed from the THz waveforms displayed in Fig. 2(a). The solid line is the experimental data, while the dashed line is the simulation obtained with the model described in [23].

5. Conclusions and future outlook

We studied the broadband coherent THz emission from a laser-induced microplasma. The radiation can be visualized as a forward propagating cone with a very high divergence angle. The THz emission is locally linearly polarized, and oscillating in the plane defined by the laser excitation propagation axis and the local THz propagation axis. The radiation pattern can be explained within the framework of transition-Cherenkov-like emission, which remarkably provides a qualitative description of the THz radiation from "one color" plasmas over more than seven order of magnitude differences in plasma length, from tenths of micron to tenths of centimeter. The coherent nature of the emission suggests that more complicated, even arbitrary, radiation patterns might be achieved by combining the radiation from multiple microplasmas, similarly to a phase array.

We measured THz waveforms generated with laser pulse energies as low as 660 *nJ*, which, to our knowledge, is the lowest reported laser pulse energy for THz generation in ambient air. A simple strategy to improve the SNR significantly at this low value of laser energy is to use laser sources with higher repetition rate, resulting in an increased number of measured pulses in the unit of time. Since the SNR is expected to grow as the square root of the repetition rate, by employing lasers sources working at hundreds of Hertz, we expect the SNR to be improved by more than one order of magnitude.

Further optimization of the technique, including improved design of the THz collection optics, the use of the two-color approach, of longer excitation laser wavelengths and shorter pulse durations, has the promise to untap the full potential of plasma-based THz techniques with low energy ultrafast lasers.

Acknowledgments

The authors thank US Army Research Office for the financial support.

References

[1] Kolner, B. H., Buckles, R. A., Conklin, P. M. et al. "Plasma Characterization With Terahertz Pulses". *IEEE J. Sel. Top. Quantum Electron.* 14, 505–512 (2008).

[2] Jepsen, P. U., Cooke, D. G. & Koch, M. "Terahertz spectroscopy and imaging - Modern techniques and applications". *Laser Photonics Rev.* 5, 124–166 (2011).

[3] Ulbricht, R., Hendry, E., Shan, J., et al. "Carrier dynamics in semiconductors studied with time-resolved terahertz spectroscopy". *Rev. Mod. Phys.* 83, 543–586 (2011).

[4] McIntosh, A. I., Yang, B., Goldup, S. M., et al. "Terahertz spectroscopy: a powerful new tool for the chemical sciences"? *Chem. Soc. Rev.* 41, 2072 (2012).

[5] Nuss, M., Auston, D. & Capasso, F. "Direct Subpicosecond Measurement of Carrier Mobility of Photoexcited Electrons in Gallium Arsenide". *Phys. Rev. Lett.* 58, 2355–2358 (1987).

[6] Exter, M. van, Fattinger, C. & Grischkowsky, D. "Terahertz time-domain spectroscopy of water vapor". *Opt. Lett.* 14, 1128 (1989).

[7] Dai, J., Xie, X. & Zhang, X.-C. "Detection of Broadband Terahertz Waves with a Laser-Induced Plasma in Gases". *Phys. Rev. Lett.* 97, (2006).

[8] Karpowicz, N. et al. "Coherent heterodyne time-domain spectrometry covering the entire ‘terahertz gap’". *Appl. Phys. Lett.* 92, 011131 (2008).

[9] Liu, J. & Zhang, X. C. "Birefringence and absorption coefficients of alpha barium borate in terahertz range". *J. Appl. Phys.* 106, 023107 (2009).

[10] Zalkovskij, M. et al. "Ultrabroadband terahertz spectroscopy of chalcogenide glasses". *Appl. Phys. Lett.* 100, 031901 (2012).

[11] D’Angelo, F., Mics, Z., Bonn, M. et al. "Ultra-broadband THz time-domain spectroscopy of common polymers using THz air photonics". *Opt. Express* 22, 12475 (2014).

[12] McLaughlin, C. V. et al. "Wideband 15 THz response using organic electro-optic polymer emitter-sensor pairs at telecommunication wavelengths". *Appl. Phys. Lett.* 92, 151107 (2008).

[13] Matsubara, E., Nagai, M. & Ashida, M. "Ultrabroadband coherent electric field from far infrared to 200 *THz* using air plasma induced by 10 *fs* pulses". *Appl. Phys. Lett.* 101, 011105 (2012).

[14] Clerici, M. et al. "Wavelength Scaling of Terahertz Generation by Gas Ionization". *Phys. Rev. Lett.* 110, (2013).

[15] Hamster, H., Sullivan, A., Gordon, S., et al. "Subpicosecond, electromagnetic pulses from intense laser-plasma interaction". *Phys. Rev. Lett.* 71, 2725–2728 (1993).

[16] Cook, D. J. & Hochstrasser, R. M. "Intense terahertz pulses by four-wave rectification in air". *Opt. Lett.* 25, 1210 (2000).

[17] Kress, M., Torsten Löffler, Eden, S., Thomson, M. et al. "Terahertz-pulse generation by photoionization of air with laser pulses composed of both fundamental and second-harmonic waves". *Opt. Lett.* 29, 1120 (2004).

[18]Xie, X., Dai, J. & Zhang, X.-C. "Coherent Control of THz Wave Generation in Ambient Air". *Phys. Rev. Lett.* 96, (2006).

[19] Buccheri, F. & Zhang, X.-C. "Terahertz emission from laser-induced microplasma in ambient air". *Optica* 2, 366 (2015).

[20] Wu, Q. & Zhang, X.-C. "Free-space electro-optic sampling of terahertz beams". *Appl. Phys. Lett.* 67, 3523 (1995).

[21] Sato, M. et al. "Terahertz polarization pulse shaping with arbitrary field control". *Nat. Photonics* 7, 724–731 (2013).

[22] Hamster, H., Sullivan, A., Gordon, S. et al. "Short-pulse terahertz radiation from high-intensity-laser-produced plasmas". *Phys. Rev. E* 49, 671–677 (1994).

[23] Amico, C. D. et al. "Forward THz radiation emission by femtosecond filamentation in gases: theory and experiment". *New J. Phys.* 10, 013015 (2008).